

A biaxial nematic gel phase in aqueous vanadium pentoxide suspensions

O. Pelletier¹, C. Bourgaux², O. Diat³, P. Davidson^{1,a}, and J. Livage⁴

¹ Laboratoire de Physique des Solides^b, Bâtiment 510, Université Paris-Sud, 91405 Orsay Cedex, France

² Laboratoire pour l'Utilisation du Rayonnement Électromagnétique^c, Université Paris-Sud, 91405 Orsay Cedex, France

³ ESRF, B.P. 220, 38043 Grenoble Cedex, France

⁴ Laboratoire de Chimie de la Matière Condensée^d, Université Pierre et Marie Curie, 4 Place Jussieu, 75252 Paris, France

Received 26 May 1999

Abstract. Aqueous suspensions of V_2O_5 ribbons are one of the very few examples of mineral liquid crystals. In the concentrated regime, we show that these ribbons organize in a biaxial nematic gel phase. A Couette shear cell was used to produce a well oriented sample for *in situ* synchrotron X-ray scattering studies. We observed two perpendicular anisotropic sections of reciprocal space, which proves the biaxial symmetry of the nematic order. The thermodynamic and flow properties of the biaxial nematic are well described by hard-core theories. We suggest the use of a shear geometry to produce and investigate single domains of other biaxial nematics, reported but still questioned in the literature.

PACS. 61.10.Eq X-ray scattering (including small-angle scattering) – 61.30.-v Liquid crystals – 64.70.Md Transitions in liquid crystals

1 Introduction

Nematic liquid crystals are fluids made of anisotropic molecules oriented on average along a preferred direction which is an axis of symmetry for the system. This axis can be of infinite order, in which case the phase is an uniaxial nematic (N_u), or of finite order, in which case the phase is a biaxial nematic (N_b). The overwhelming majority of experimental systems belong to the first category: in fact, extremely few biaxial nematics have been reported in the literature [1–9] and some of the reports dealing with thermotropic liquid crystals have since been questioned [10]. The rare unambiguous examples of biaxial nematics belong either to the class of lyotropic liquid crystals made of biaxial micelles of surfactants or to that of thermotropic liquid crystalline polymers. On the theoretical side, the existence of N_b phases has been predicted by Freiser in 1970 [11]. More recent theoretical approaches [12] use “hard core” models where ordering stems from excluded volume interactions to compute “*ab initio*” phase diagrams and transport coefficients. However, the few biaxial nematics reported so far can hardly be regarded as hard core fluids. They are

dense phases in which the moieties (micelles or polymers) are close packed so that many interactions are involved, some of them being attractive. In this work, we consider a new colloidal system of ribbon-like mineral particles. This system is made of anisotropic and fairly rigid vanadium pentoxide (V_2O_5) ribbons dispersed in water [13]. Recent USAXS experiments have shown that these ribbons are 1 nm thick, 25 nm wide and 250 nm long [14]. The suspensions exhibit an isotropic (I)/ N_u phase transition at low volume fractions ($\phi \simeq 0.5\%$) well described by the Onsager theory of nematic ordering. This suggests that excluded volume is the dominant interaction. At larger volume fractions ($\phi \simeq 1.5\%$), they undergo a transition from a sol to a physical gel which is still nematic. The striking biaxiality of these mineral ribbons prompted us to investigate the concentrated part of their phase diagram, where a N_b phase may be expected. Indeed, the swelling behaviour (average distance d between particles *versus* ϕ) of these suspensions (Fig. 1), determined by small angle X-ray scattering (SAXS) experiments performed on “powder” (*i.e.* unaligned) samples, strongly suggested its existence [13]. At volume fractions larger than 4%, a peculiar 1-dimensional (1D) swelling law had been observed whereas the swelling law was 2-dimensional (2D) at lower volume fractions as expected for a common N_u phase. This crossover occurs when the average distance between ribbons becomes comparable to

^a e-mail: davidson@lps.u-psud.fr

^b UMR 8502

^c UMR 130

^d URA 1466

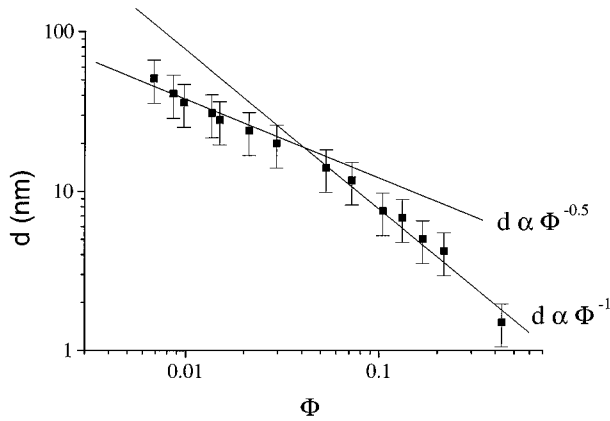


Fig. 1. Swelling behaviour of the V_2O_5 suspensions.

their width which indicates a rotational hindrance in the concentrated regime.

However, investigating the biaxiality of a nematic sample requires either the structural study of a single domain (or at least of a well oriented sample), or the presence of suitable nuclei to perform NMR experiments [9,10] (in which case one needs a sample randomly aligned at least in two dimensions) or the detailed study of optical textures in polarized light microscopy [8]. This latter technique could not be used with V_2O_5 suspensions because they are much too absorbent and because the defect density is too large. Vanadium NMR is dominated by the presence of paramagnetic V^{IV} species and is therefore of no help. Producing an aligned sample is not straightforward either. A solution sometimes consists in the simultaneous application of magnetic and electric fields but V_2O_5 suspensions at these concentrations do not align in fields due to their viscoelastic properties. We thus had to devise a new way to achieve biaxial orientation. Shearing was previously shown to orient these suspensions with the long axes of the ribbons aligned along the direction of shear [13]. A shear geometry, being biaxial, can reveal the intrinsic biaxial symmetry of the concentrated samples. We have therefore performed SAXS experiments under shear on two nematic gel samples of volume fractions 5% and 2% belonging respectively to the 1D and 2D swelling regimes. We will show that shearing is indeed an effective way of achieving biaxial alignment of the ribbons and that concentrated V_2O_5 suspensions form a biaxial nematic gel phase. Moreover, this new N_b phase has thermodynamic and flow properties that agree with hard core theories of N_b phases.

2 Experimental

V_2O_5 suspensions were synthesized by a sol-gel process described in detail elsewhere [13]. Their concentration was determined by the weight loss upon calcination with an accuracy better than 0.2%. Samples were then prepared to the desired concentration by slowly drying the original dispersions. Concentrated samples were stirred to ensure homogeneity. We have used a Couette shear cell (Fig. 2a)

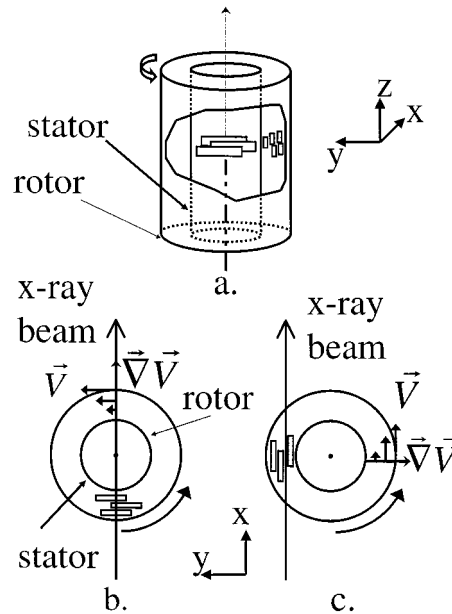


Fig. 2. a) 3D view of the Couette cell with a schematic drawing of the organization of the biaxial nematic phase of V_2O_5 ribbons. b) top view of the Couette cell in the radial configuration (RC). c) top view of the Couette cell in the tangential configuration (TC).

especially designed for *in situ* SAXS experiments, consisting in two coaxial polycarbonate cylinders. The sample is inserted into the gap between the cylinders; the outer one is the rotor and the inner one is the stator.

Two scattering experiments with a different symmetry axis aligned along the X-ray beam are necessary to demonstrate the biaxial symmetry of a nematic sample. Since we cannot rotate the Couette cell with respect to the beam, we worked in two distinct configurations (Figs. 2b and 2c). For clarity, the ribbons are depicted with their long axes oriented on average along the flow as it was deduced from the experimental results described below. The X-ray beam is perpendicular to the flow lines in the radial configuration (RC) and is parallel to them in the tangential configuration (TC). The combination of two RC and TC experiments is thus well suited to investigate the existence of a N_b phase. In order to obtain clear scattering patterns in the TC, an X-ray beam of diameter smaller than the gap is required. Moreover, to overcome the stronger absorption in this configuration, we used a high energy (12.4 keV) and high flux monochromatic beam (10^{12} ph/s in $200 \times 200 \mu\text{m}^2$) on the “high brilliance” ID2 beamline at the ESRF (European Synchrotron Radiation Facility, Grenoble France) [15]. The implementation of this Couette shear cell on a high brilliance synchrotron X-ray line has already proved a very powerful technique to study shear flow of complex fluids [16,17].

3 Results

Figure 3 shows the results obtained with the 5% and 2% samples. Scattering patterns recorded in the RC both

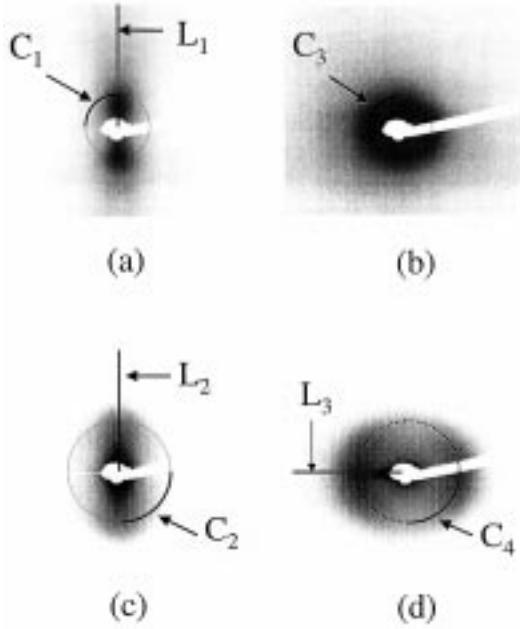


Fig. 3. 2-D scattering patterns obtained - with the 2% sample: (a) in the RC, (b) in the TC - with the 5% sample: (c) in the RC, (d) in the TC.

show a clear anisotropy (Figs. 3a and 3c), with the intensity localized along the Oz direction. This shows that, as expected, the ribbons are aligned with their long axes parallel to the flow in both samples. Now, scattering patterns taken in the TC directly assess the uniaxial or biaxial character of the nematic order. The 2% sample shows complete revolution symmetry around its director (Fig. 3b): it is uniaxial. It should be noted here that this sample remained uniaxial even under the largest shear rate available, *i.e.* 8000 s^{-1} . In contrast, the 5% sample does not show this rotational symmetry (Fig. 3d): it is biaxial. This orientation can be produced by applying a shear rate as low as 100 s^{-1} during 5 minutes. The orientation does not relax and the order parameter V remains constant upon cessation of shear on the time scale of a SAXS experiment, *i.e.* hours. The reproducibility of all the experiments described here was systematically checked.

More quantitative insight into the organization of the ribbons can be drawn from azimuthal and radial cuts of the scattered intensity along different paths (L_{1-3} , C_{1-4} , Fig. 3). Let us first describe the orientational order more quantitatively. Two directors are classically used to define the orientation of a N_b phase. The “main” director, called \bar{n} , gives the direction of the long axes of the particles whereas the “biaxial” director, called \bar{m} , gives the direction of the transverse axes of the particles, along their breadth. A set of 4 scalar order parameters is also introduced [18] as the averages of different functions of the Euler angles (α, β, γ) that a ribbon shaped particle makes with a reference frame, weighted by the orientational distribution function $f(\alpha, \beta, \gamma)$. Only two of these parameters are relevant in our case. One is the well known order parameter $S = \langle \frac{3 \cos^2 \alpha - 1}{2} \rangle$ which describes the orienta-

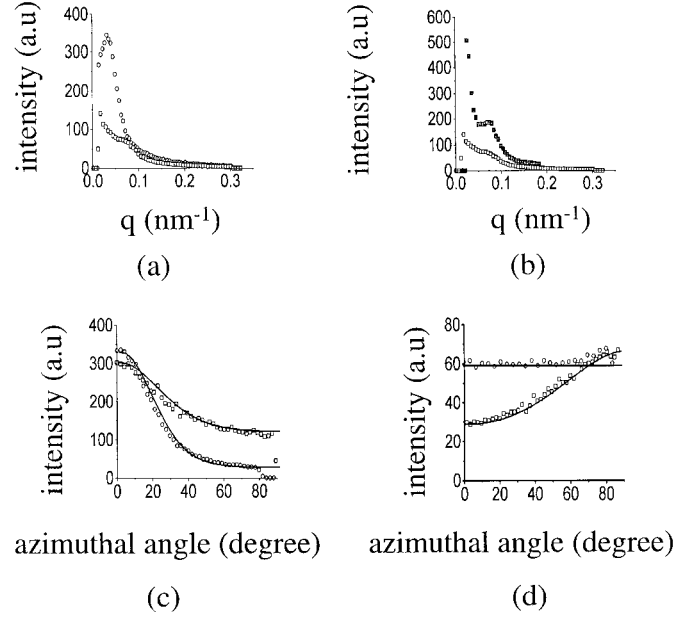


Fig. 4. X-ray intensity (in arbitrary units) – versus scattering vector s ($s = \frac{2}{\lambda} \sin \frac{\theta}{2}$ with λ the wavelength and θ the scattering angle) in nm^{-1} (a) along L_1 (open circles) and L_2 (open squares), (b) along L_2 (open squares) and L_3 (filled squares) – versus azimuthal angle (c) along C_1 (open circles) and C_2 (open squares), (d) along C_3 (open circles) and C_4 (open squares). Solid lines are fits (see text).

tional order of the long axes of the ribbons. It is the only non-zero order parameter in the N_u phase. The other one is $V = \frac{1}{2} \langle (1 + \cos^2 \alpha) \cos 2\beta \cos 2\gamma - \cos \alpha \sin 2\beta \sin 2\gamma \rangle$ which describes the biaxial order. The measurement of S in the N_u phase is straightforward. The intensity scattered on circle C_1 is classically modelled [19] by the formula: $I(\theta) = k \frac{e^{m \cos^2 \theta}}{\sqrt{m} \cos \theta} \text{erf}(\sqrt{m} \cos \theta)$, where k is a normalization factor, erf is the error function, θ is the azimuthal angle and m is a fit parameter directly related to S . Fitting the scattered intensity with this formula yields $S \simeq 0.75$, in good agreement with previous experiments on magnetically aligned samples [20]. Unfortunately, several assumptions involved in this procedure are not met by the N_b phase. Nevertheless, we have fitted the azimuthal cut C_2 using the same formula (Fig. 4c). The fit is still accurate and yields $S \simeq 0.5$ in the N_b phase. Additional experiments are needed to confirm this decrease of S at the N_u/N_b transition, which seems rather surprising when compared to computer simulations [21]. This effect could simply be due to a remaining mosaic spread of the sample but the onset of biaxial ordering might also decrease the value of S [22].

To our knowledge, there is no analytical expression for the intensity scattered by a biaxial nematic allowing the determination of V so that we had to resort to a very pragmatic approach. We have assumed that the long axes of the ribbons were perfectly oriented. Then, the intensity scattered along C_4 is proportional to the convolution product of the orientational distribution function of \bar{m}

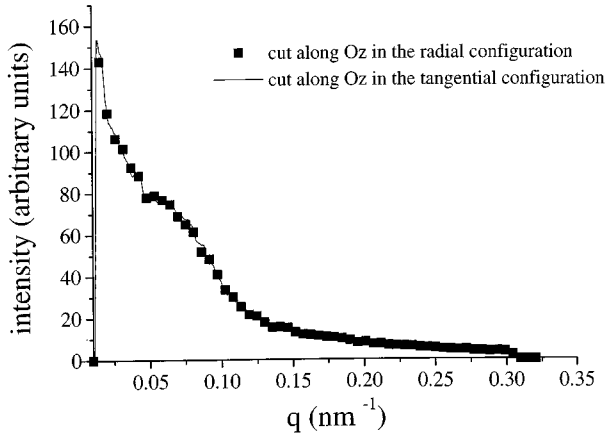


Fig. 5. X-ray intensity along Oz versus scattering vector s in nm^{-1} for the 5% sample in RC and TC. The intensities are given in number of counts divided by the absorption coefficient of the sample measured in each configuration and by the exposure time.

(supposed to be confined in a plane perpendicular to \bar{n}) by a Gaussian intensity distribution accounting for the finite width of the ribbons. Assuming a Maier-Saupe form ($e^{m \cos^2 \phi}$) [23] for the orientational distribution function of \bar{m} , we have performed a fit which leads to $V \simeq 0.35 \pm 0.05$ for the 5% sample (Fig. 4d). It is clear that V is lower than S in the N_b phase. To check the validity of this treatment, we have applied it to the 2% sample (along C_3) and obtained $V \simeq 0 \pm 0.05$, in agreement with its uniaxial nature.

Let us now consider the local positional order as inferred from radial cuts of the scattering patterns. The two samples are obviously different in this respect. In the RC, cuts along Oz (lines L_1 and L_2) show a clear correlation peak for the 2% sample at $s \simeq 0.033 \text{ nm}^{-1}$ (where s is the scattering vector modulus) but only a very weak shoulder for the 5% sample (Fig. 4a). Once corrected for the different absorption coefficients, cuts along Oz in the TC perfectly match those in the RC, as illustrated in Figure 5. This proves that the two different sample volumes probed in each configuration actually have the same structure. In other words, the samples are homogeneous throughout the shear cell. For the 5% sample, a cut along Oy , in the TC (line L_3), shows a well defined correlation peak at $s \simeq 0.075 \text{ nm}^{-1}$ (Fig. 4b). Due to the rather low value of V , the tail of this peak gives rise to the above mentioned weak shoulder along L_2 which is located at the same value of s . These two peaks correspond to distances in real space of 30 nm and 13.5 nm for the 2% and 5% samples respectively. In the N_u phase, this distance can be understood as the average separation between the long axes of the ribbons [13]. In the N_b phase, it corresponds to the average distance between their flat faces. The normal to these faces is oriented along the velocity gradient as shown schematically in Figure 2. There does not seem to be any lateral ordering of the ribbons (along Oz) in the biaxial phase because we do not observe any additional peak in this direction and because the scattering is well described by the form factor of the ribbons instead.

4 Discussion

Our experimental results can be interpreted by assuming that V_2O_5 ribbons are plain parallelepipeds interacting essentially through hard core repulsion. Their surface charge is highly screened because the Debye length is around 3 nm at the ionic strength $I = 10^{-2}$ of the suspensions. The experimental phase sequence: $I/N_u/N_b$ as concentration increases is that predicted by hard core theories and numerical simulations [12]. Moreover, the I/N_u transition is found strongly first order whereas the N_u/N_b transition is at most weakly first order, a fact also theoretically expected. More precisely, recent models [12] do indeed predict a N_u/N_b phase transition for such systems at high enough concentrations under the following conditions: the dimensions (a , b and c) of the parallelepiped must correspond to the so-called self-conjugate point where $b = \sqrt{ac}$ (where a Landau bicritical point is expected), and a smectic phase must not be more stable than the N_b phase. The last condition is easily met by our system because of the intrinsic polydispersity of the ribbons (the slightest degree of polydispersity is known to prevent smectic ordering). Moreover, the width of the ribbons (25 nm) is somewhat larger than the one that would correspond to the self-conjugate shape (17 nm). This is still close enough for a N_b phase to be stable, but then the I/N_u and N_u/N_b transitions are predicted to occur at very different concentrations, so that the uniaxial phase at the N_u/N_b transition should be well ordered. The biaxial director \bar{m} is thus nearly confined in a plane, and the uniaxial/biaxial transition can be seen as an isotropic/nematic transition in 2 dimensions for the director \bar{m} . Very simple arguments (similar to those giving the scaling of the volume fraction at the transition for the Onsager theory of uniaxial nematic ordering) can now be used to estimate the volume fraction ϕ_b at this transition. The order of magnitude of ϕ_b is obtained from the condition of overlap of the excluded areas of the cross sections of the ribbons. This leads to $\phi_b \propto \frac{\text{thickness}}{\text{width}} \simeq 4\%$ (within a multiplicative factor of order unity), again in good agreement with our experimental data. Let us note that even though the Onsager theory is strongly first order in 3 dimensions, its extensions to 2 dimensions give a second order phase transition [24–26]. Therefore the idea of a second “Onsager like” phase transition for the director \bar{m} seems to give a qualitative picture of the situation both in terms of volume fraction and order parameter at the transition.

We now discuss the positional short-range order of the ribbons. First, let us recall however that the nature of the biaxial nematic phase is only defined by the symmetries of the long range orientational order [27,28]. This means that the properties of the short range positional order are actually irrelevant in this respect. Nevertheless, the close examination of the positional correlations in this biaxial nematic gel phase is instructive. A common idea of a biaxial nematic phase is that it should display three different scattering peaks along its three main axes (let us note by the way that the observation of three peaks at different s values in the scattering of unoriented samples does not prove in any way the biaxial nature



Fig. 6. Schematic representation of the organization of the ribbons in a plane perpendicular to the first director \bar{n} . The straight segments represent the cross-sections of the ribbons. \bar{m} is oriented along a diagonal of the figure.

of the phase examined). This idea may be valid for dense biaxial nematic phases such as a thermotropic biaxial nematic or for the lyotropic biaxial nematics of micelles which have relatively little water. In such cases, the building blocks are very close to each other or even in contact, so that their separation cannot fluctuate very much. Therefore, short range positional correlations are then readily observed. The V_2O_5 suspensions examined in this work are very different because they are composed of 95% water and only 5% of V_2O_5 ribbons. The distances between ribbons can fluctuate much more. For instance, considering the width of the peak in Figure 4b, it is clear that the average distance between the flat faces of the ribbons fluctuates by at least 30%. Similarly, still in the plane perpendicular to \bar{n} , the average distance between ribbon edges must fluctuate even more because there is no reason why the short sides of the ribbons should be in register. This explains why no lateral short-range positional correlations between ribbons can be observed. A schematic representation of the organization of this biaxial nematic gel phase is shown in Figure 6. To conclude on this particular point, the absence of lateral short-range positional order does not conflict with the biaxial symmetry of the phase but should rather be considered as a distinctive feature of this very dilute biaxial nematic gel phase.

The orientation of our shear-aligned samples is another interesting feature that can be accounted for by theories. Leslie *et al.* [29] have developed a general framework to discuss the stability under flow of a given orientation depending on the value of three coefficients τ_1 , τ_2 , τ_3 . These coefficients have been calculated by Fialkowski [30] for a biaxial nematic phase of hard parallelepipeds of dimensions a , b , c ($a < b < c$). In our case, all of them are found to be negative and of absolute value larger than unity. For such a set of coefficients, the only stable orientation predicted by Leslie *et al.* is that for which \bar{m} is oriented along the neutral axis z and \bar{n} is in the direction of flow. This is precisely the orientation observed experimentally.

These SAXS studies show unambiguously that V_2O_5 gels at 5% volume fraction have a biaxial nematic order. Besides, their properties are well described by recent hard-

core theories. However, the gel nature of these materials raises more subtle questions about the thermodynamic nature of this biaxial nematic ordering. Shearing these suspensions is known to suppress their elastic properties but one may wonder if any relaxation of the biaxial nematic order could be hampered by the gel reconstruction. At this point, it should be stressed that biaxial nematic ordering has never been observed whatever the shear rate with the suspensions of 2% volume fraction, even though they are gels too. More detailed experiments are probably needed to clarify this delicate point. In conclusion, the use of mineral compounds [31] instead of organic ones gives access to moieties which perfectly match the criteria required to observe a N_b phase both in terms of particle dimensions and interactions. To our knowledge, applying a shear stress to align a biaxial nematic sample had not yet been reported. This method should be in principle easy to apply to any kind of sample and we suggest its use to investigate other N_b phases reported but still questioned in literature.

The authors are indebted to W.M. Gelbart, R. Kamien and A.M. Levelut for helpful and pleasant discussions and thank ESRF for the award of the beamtime (SC395). We thank the referees of this article for providing us some references and for useful comments.

References

1. L.J. Yu, A. Saupe, *Phys. Rev. Lett.* **45**, 1000 (1980).
2. A.M. Figueiredo Neto, Y. Galerne, A.M. Levelut, L. Liebert, *J. Phys. Lett. France* **46**, 499 (1985).
3. A.H. Windle, C. Viney, R. Golombok, A.M. Donald, G.R. Mitchell, *Faraday Discuss. Chem. Soc.* **79**, 55 (1985).
4. J. Malthête, L. Liebert, A.M. Levelut, Y. Galerne, C. R. Acad. Sci. (Paris) II **303**, 1073 (1986).
5. F. Hessel, H. Finkelmann, *Polym. Bull.* **15**, 349 (1986).
6. S. Chandrasekhar, B.R. Ratna, B.K. Sadashiva, V.N. Raja, *Mol. Cryst. Liq. Cryst.* **165**, 123 (1988).
7. K. Praefcke, B. Kohne, B. Gündogan, D. Demus, S. Diele, G. Pelzl, *Mol. Cryst. Liq. Cryst. Lett.* **7**, 27 (1990).
8. T. De'Neve, M. Kléman, P. Navard, *J. Phys. II France* **2**, 187 (1992).
9. Per-Ola Quist, *Liq. Cryst.* **18**, 623 (1995) and references therein.
10. a) S.M. Fan, I.D. Fletcher, B. Gündogan, N.J. Heaton, G. Kothe, G.R. Luckhurst, K. Praefcke, *Chem. Phys. Lett.* **204**, 517 (1993); b) J.R. Hughes, G. Kothe, G.R. Luckhurst, J. Malthête, M.E. Neubert, I. Shenouda, B.A. Timimi, M. Tittelbach, *J. Chem. Phys.* **107**, 9252 (1997).
11. M.J. Freiser, *Phys. Rev. Lett.* **24**, 1041 (1970).
12. a) B.M. Mulder, *Phys. Rev. A* **39**, 2742 (1989); b) M.P. Allen, *Liq. Cryst.* **8**, 499 (1990); c) M.P. Taylor, J. Herzfeld, *Phys. Rev. A* **44**, 3742 (1991); d) S. Sarman, *J. Chem. Phys.* **107**, 3144 (1997).
13. P. Davidson, C. Bourgaux, L. Schouffeten, P. Sergot, C. Williams, J. Livage, *J. Phys. II France* **5**, 1577 (1995).
14. O. Pelletier, C. Bourgaux, O. Diat, P. Davidson, J. Livage, *Eur. Phys. J. B* (submitted).
15. P. Bösecke, O. Diat, *J. Appl. Cryst.* **30**, 867 (1997).

16. F.R. Melino, J.F. Berret, G. Porte, O. Diat, P. Lindner, Eur. Phys. J. B **3**, 59 (1998).
17. I.W. Hamley, J.A. Pople, J.P.A. Fairclough, N.J. Terrill, A.J. Ryan, C. Booth, G.E. Yu, O. Diat, K. Almdal, K. Mortensen, M. Vigild, J. Chem. Phys. **108**, 6929 (1998).
18. J.P. Straley, Phys. Rev. A **10**, 1881 (1974).
19. P. Davidson, D. Petermann, A.M. Levelut, J. Phys. II France **5**, 113 (1995).
20. X. Commeinhes, P. Davidson, C. Bourgaux, J. Livage, Adv. Mater. **9**, 900 (1997).
21. G.R. Luckhurst, S. Romano, Mol. Phys. **40**, 129 (1980).
22. W.M. Gelbart, J. Phys. Chem. **86**, 4298 (1982).
23. Another form for the distribution function in 2 dimensions can be found. It is $e^{m \cos 2\phi}$. It is mathematically equivalent to the one we use.
24. R.F. Kayser, H.J. Raveché, Phys. Rev. A **17**, 2067 (1978).
25. Z.Y. Chen, Phys. Rev. Lett. **71**, 93 (1993).
26. P. van der Schoot, J. Chem. Phys. **106**, 2355 (1997).
27. J. Prost, P.G. de Gennes, *The Physics of Liquid Crystals* (Oxford University Press, Oxford, 1993).
28. P.M. Chaikin, T.C. Lubensky, *Principles of Condensed Matter Physics* (Cambridge University Press, Cambridge, 1995).
29. a) F.M. Leslie, J.S. Lavery, T. Carlsson, Quart. J. Mech. Appl. Math. **45**, 595 (1992); b) T. Carlsson, F.M. Leslie, J.S. Lavery, Mol. Cryst. Liq. Cryst. **210**, 95 (1992).
30. M. Fialkowski, Phys. Rev. E. **55**, 2902 (1997).
31. For a recent review on mineral liquid crystal see: a) P. Davidson, P. Batail, J.C.P. Gabriel, J. Livage, C. Sanchez, C. Bourgaux, Prog. Polym. Sci. **22**, 913 (1997); b) J.C.P. Gabriel, P. Davidson, Adv. Mater. (in press).